Turkish Journal of Chemistry

Volume 42 | Number 2 Article 24

1-1-2018

Multiwall carbon nanotube paste electrode as a sensor for sensitive determination of deferasirox in the presence of uric acid: application for the analysis of pharmaceutical and biological samples

GOLNAZ PARVIZI FARD

REZA EMAMALI SABZI

TÜBİTAK

Turkish Journal of Chemistry

http://journals.tubitak.gov.tr/chem/

Research Article

Turk J Chem
(2018) 42: 493 – 504

doi:10.3906/kim-1707-9

Multiwall carbon nanotube paste electrode as a sensor for sensitive determination of deferasirox in the presence of uric acid: application for the analysis of pharmaceutical and biological samples

Golnaz PARVIZI FARD[1], **Reza EMAMALI SABZI**[1,2,*]
[1]Department of Analytical Chemistry, Faculty of Chemistry, Urmia University, Urmia, Iran
[2]Institute of Biotechnology, Urmia University, Urmia, Iran

Received: 03.07.2017 • **Accepted/Published Online:** 19.12.2017 • **Final Version:** 27.04.2018

Abstract: In this work, the electrochemical oxidation of deferasirox at a multiwall carbon nanotube paste electrode (MWCNTPE) was described. The electrochemical behavior of deferasirox was studied using cyclic voltammetry and chronoamperometry techniques and parameters such as charge transfer coefficient (α), the number of electrons involved in the rate-determining step (n_a), and diffusion coefficient (D) were calculated. The capability of the electrode for the determination of deferasirox at low concentrations was investigated using the differential pulse voltammetry technique. It was found that the calibration graph of deferasirox was linear in the concentration range of 0.16–16.5 μM and its detection limit was determined to be approximately 0.1 μM. The diffusion coefficient was calculated to be 1.8×10^{-6} cm^2 s^{-1} for deferasirox. The differential pulse voltammetry method could be used as an effective technique for the determination of deferasirox at the MWCNTPE in the presence of uric acid. The MWCNTPE was successfully used as a sensor for sensitive detection of deferasirox in pharmaceutical and biological samples.

Key words: Multiwall carbon nanotube paste electrode, deferasirox, cyclic voltammetry, chronoamperometry, differential pulse voltammetry, electrochemical detection

1. Introduction

Deferasirox [4-[(3*Z*,5*E*)-3,5-bis(6–oxo–1–cyclohexa-2,4-dienylidene)-1,2,4–triazolidin-1-yl]benzoic acid is an oral iron chelator and is a tridentate ligand with high affinity for binding to iron(III) with a metal-to-ligand ratio of 2:1.[1] Deferasirox is a novel synthetic drug and its main application is reducing chronic iron overload in patients undergoing numerous blood transfusions due to conditions such as beta-thalassemia, sickle cell disease, and other chronic anemias.[1,2]

Iron overload can damage the liver, myocardium, spleen, and endocrine system over time.[3,4] Therefore, maintaining safe iron concentrations in tissues is very important, and this can be achieved via chelation treatment.[5] However, like many other drugs, overdose of deferasirox can occur, which could be extremely dangerous. In the case of overdose, patients suffer from severe side effects such as loss of appetite, yellow eyes or skin, vomiting, diarrhea, and unusual bleeding or bruising.

Drug analysis of pharmaceutical and biological samples has significant effects on public health. To our knowledge, limited research has been reported on the analysis of deferasirox. Some analytical methods such as liquid chromatography, spectroscopy, and spectrofluorometry have been reported for the determination of

*Correspondence: rezasabzi@yahoo.com

deferasirox.[1,2,6–12] However, these methods are time-consuming or solvent usage-intensive. Compared with other methods, electrochemical techniques, which offer faster, cheaper, and safer analysis methods, have drawn much attention and have been used for the determination of a wide range of pharmaceuticals.[13–16] A limited number of electrochemical methods have been reported for determining deferasirox.[17–19]

Carbon paste electrodes (CPEs) have several advantages over other carbonaceous or noble metal electrodes such as low background current, feasibility of incorporating different modifiers during paste preparation, easy preparation methods, simple surface renewal, low cost, and potential of miniaturization.[19] To date, different types of carbonaceous materials such as graphite, acetylene black, carbon nanofibers, carbon microspheres, and carbon nanotubes have been used in the preparation of CPEs.[21–24]

Nanotechnology has become one of the most interesting fields in science and technology.[25] Carbon nanotubes are important nanostructures due to their unique properties including tensile strength one hundred times that of steel, high thermal conductivity, high mechanical strength, electrical conductivity similar to copper, and capability of carrying much higher currents.[25–29]

In this paper, we have focused on the electrochemical oxidation of deferasirox at a multiwall carbon nanotube paste electrode (MWCNTPE) using cyclic voltammetry (CV) and chronoamperometry techniques. We have also discussed the capability of this electrode for sensitive determination of deferasirox using differential pulse voltammetry. Finally, we have used the MWCNTPE as a sensor for determining deferasirox in pharmaceutical and biological samples.

2. Results and discussion

2.1. Surface morphology of the MWCNTPE and CPE

Scanning electron microscopy was employed to characterize the surfaces of both the MWCNTPE and CPE as shown in Figure 1. For CPE (Figure 1A), a dense, scaly, and porous surface appeared with separated carbon layers due to the heterogeneous dispersion of carbon powder, whereas for the MWCNTPE (Figure 1B), carbon nanotubes were visible at the edges of the separated carbon sheets.

2.2. Characterization of the MWCNTPE and CPE by electrochemical impedance spectroscopy

Figure 2 shows Bode (Figure 2A) and Nyquist (Figures 2B and 2C) plots for the CPE and MWCNTPE, respectively. An equivalent electrical circuit model, shown in the inset of Figure 2A, was proposed to fit the results obtained by electrochemical impedance spectroscopy (EIS) analysis. In this model, $R1$ is electrolyte resistance, $CPE1$ is the double-layer constant phase element, $R2$ is charge transfer resistance, and $W1$ is Warburg resistance, which is related to mass transfer resistance. The fitted EIS parameters are presented in Table 1.

Table 1. The fitting EIS parameters for the CPE and MWCNTPE.

Sample	R_1 (Ω cm^2)	CPE1 – P	CPE1 – T (Ω^{-1} cm^{-2} s^n)	R_2 (Ω cm^2)	W_R	Chi-square
CPE	47.54	0.94	4.96×10^{-7}	26,822	6.88×10^5	0.002235
MWCNTPE	79.86	0.77	4.52×10^{-5}	22,459	2.15×10^5	0.010223

The charge transfer resistances ($R2$) of the CPE and MWCNTPE were 26,822 and 22,459 Ω cm^2, respectively. Figure 2A clearly shows that the charge transfer resistance of the MWCNTPE was decreased.

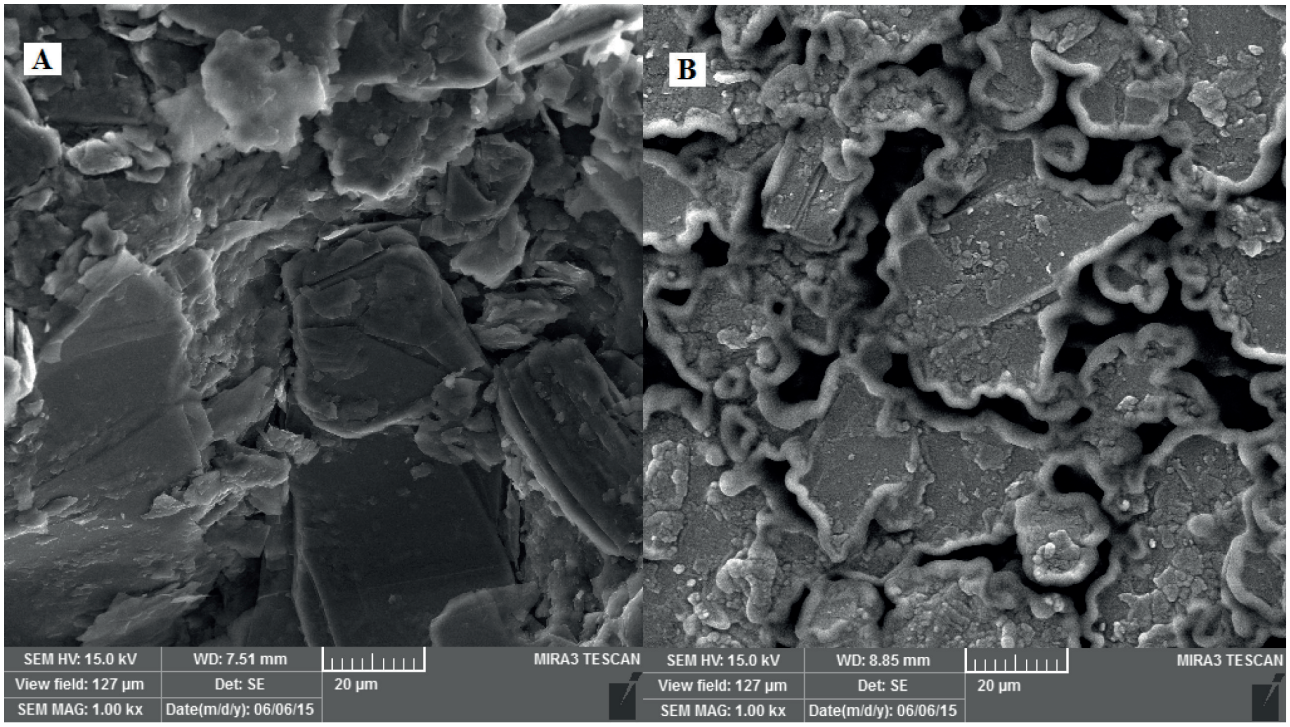

Figure 1. SEM images of a) CPE and b) MWCNTPE.

2.3. Preliminary investigation using cyclic voltammetry

A preliminary investigation using CV was conducted to evaluate the electrochemical behavior of deferasirox at the CPE. Figure 3 shows cyclic voltammograms of the CPE (curves a and b) and the MWCNTPE (curves c and d) in 0.1 M phosphate buffer solution containing 0.25 M KCl at pH 7 (as the supporting electrolyte) in the absence (a, c) and presence (b, d) of 0.4 mM deferasirox at the scan rate of 50 mV s^{-1}.

Curve a of Figure 3 is related to the CPE in the absence of deferasirox. Upon the addition of 0.4 mM deferasirox to the supporting electrolyte solution, a weak anodic peak with the potential of 0.82 V appeared at the CPE (Figure 3, curve b), with peak current of 50 μA. Curve c of Figure 3 is related to the MWCNTPE in the supporting electrolyte solution in the absence of deferasirox. Similarly, in the presence of 0.4 mM deferasirox, a sharp anodic peak with the potential of 0.65 V and peak current of 175 μA was observed at the MWCNTPE (Figure 3, curve d).

The analyzed results indicated that the MWCNTPE had excellent catalytic activity for the oxidation of deferasirox as it presented a much higher peak current at a lower peak potential (0.65 mV) compared to that obtained for the CPE.

2.4. Effect of pH

At pH levels below 5, the deferasirox solution became turbid, probably because of the low solubility of deferasirox at these pH values. At pH levels above 10, the currents of oxidation peaks of deferasirox were decreased and peak shapes were deformed. For this reason, the effect of the pH of the supporting electrolyte on the electrooxidation of deferasirox at the MWCNTPE was investigated by differential pulse voltammetry using 16 μM deferasirox in 0.1 M phosphate and 0.25 M KCl solutions at pH values of a) 5, b) 6, c) 7, d) 8, e) 9, and f) 10 (Figure 4A). The

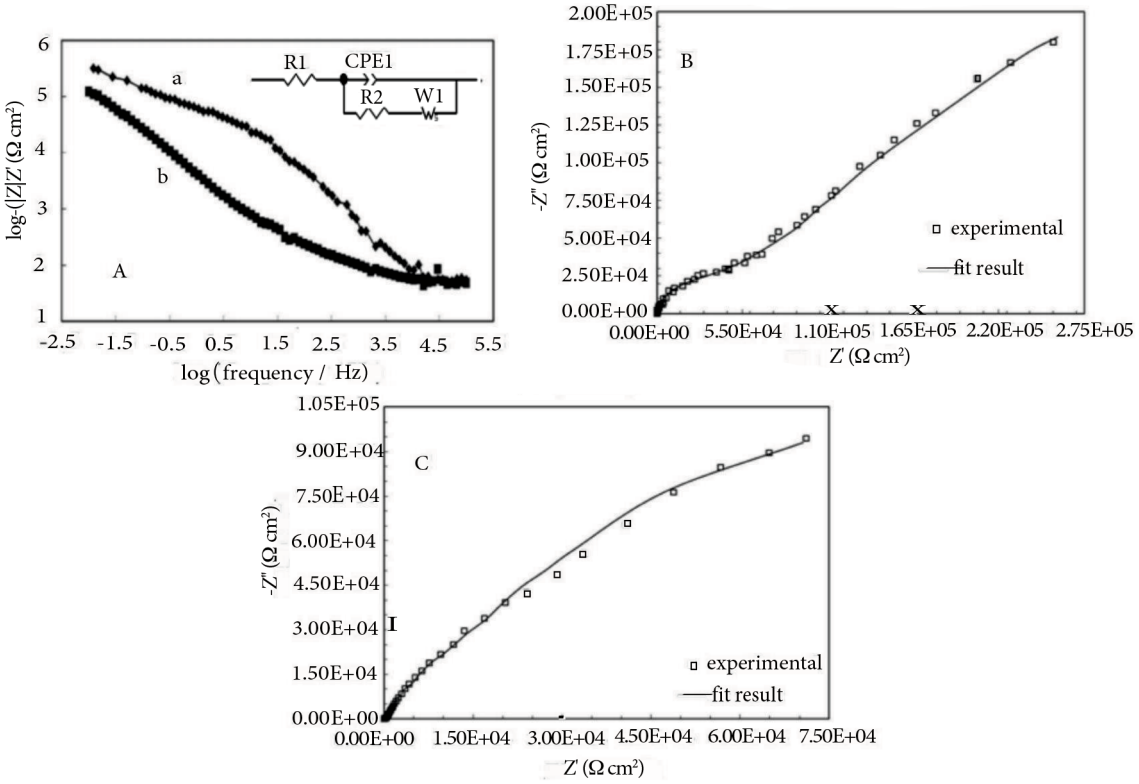

Figure 2. A) Bode plots for CPE (a) and MWCNTPE (b), and B) Nyquist plot for CPE. C) Nyquist plot for MWCNTPE in a mixture solution of 5 mM $[Fe(CN)_6]^{3-/4-}$ and 2 M KCl. Inset: Equivalent electrical circuit model.

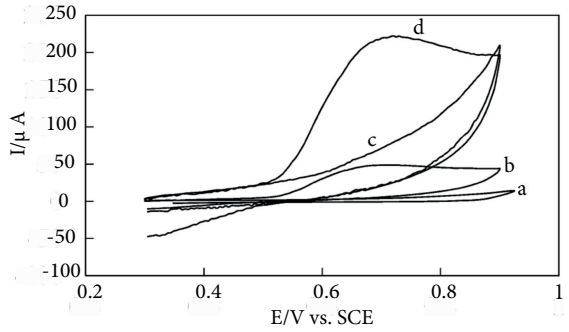

Figure 3. Cyclic voltammograms of CPE in the (a) absence and (b) presence of 0.4 Mm deferasirox and MWCNTPE in the (c) absence and (d) presence of 0.4 mM deferasirox at the scan rate of 50 mV s^{-1}. Supporting electrolyte: 0.1 M phosphate buffer solution and 0.25 M KCl (pH 7).

maximum peak current for deferasirox oxidation was obtained at pH 7 (Figure 4B). Thus, pH 7 was selected as the optimum pH for further electrochemical studies of deferasirox. Figure 4A shows that by decreasing the pH of the supporting electrolyte, the oxidation peak of deferasirox was shifted towards more positive potentials. The variation of peak potential (E_p) as a function of pH gave a straight line with a negative slope of 66 mV/pH (Figure 4C), which was closely related to the anticipated Nernstian value of 59 mV/pH at 25 °C for reactions with an equal number of protons and electrons.

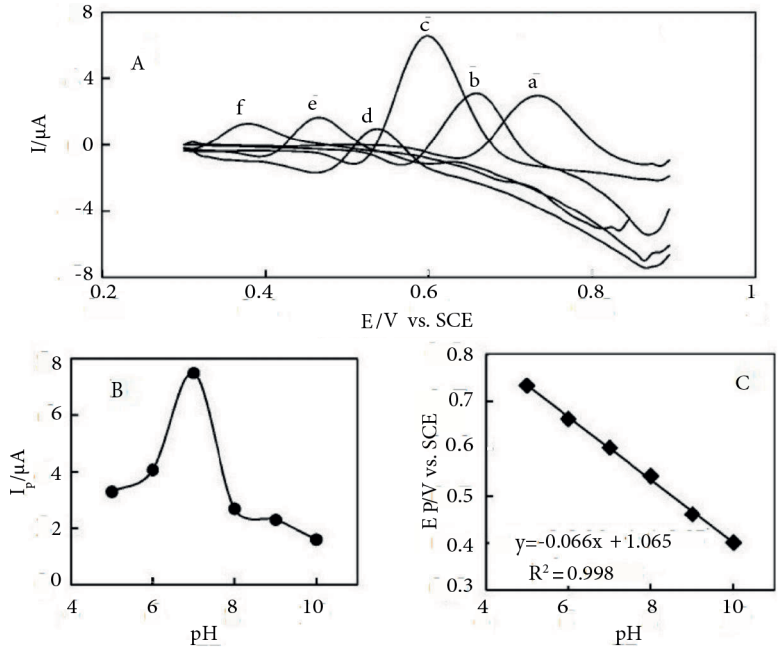

Figure 4. A) Differential pulse voltammograms of 16 μM deferasirox at MWCNTPE at various pH levels of (a) 5, (b) 6, (c) 7, (d) 8, (e) 9, and (f) 10. B) Plot of variations of peak currents versus pH. C) Plot of variations of peak potentials versus pH. Supporting electrolyte: 0.1 M PBS and 0.25 M KCl.

2.5. Effect of scan rate

Cyclic voltammetry with different potential sweep rates was used to determine the effect of scan rate on the deferasirox oxidation peak. Figure 5A shows voltammograms of 0.2 mM deferasirox in the supporting electrolyte at scan rates ranging from 10 to 500 mV s^{-1}.

At scan rates above 500 mV s^{-1} the peak of deferasirox was deformed and was not sharp enough for the determination of E_P. Since accurate evaluation of E_P was necessary for analytical applications, the effect of scan rate on the electrooxidation of deferasirox was investigated in the range of 10–500 mV s^{-1}. The oxidation peak current of deferasirox was linearly increased with the square root of the scan rate (Figure 5B), suggesting that the reaction was controlled by mass transfer. The peak potential for the oxidation of deferasirox was also shifted to more positive potentials by increasing the scan rate (Figure 5C), suggesting a kinetic limitation in the electrode reaction. In other words, by increasing the potential scan rate, the oxidation of deferasirox was accomplished at more positive potentials as a result of kinetic limitation involved in the electron-transfer reaction. The slope of variation of E_P versus log v can be used for the calculation of some kinetic parameters such as α (charge transfer coefficient) and n_a (the number of electrons involved in the rate-determining step).

To obtain information on charge transfer coefficient (α), the number of electrons involved in the rate-determining step (n_a), and the Tafel slope (b), we used Eq. (1) for electric potential (E_p), which is valid for a totally irreversible diffusion-controlled process:

$$E_P = b/2 \log \nu > +a. \tag{1}$$

Here, b is the Tafel slope, ν is the potential scan rate, and a is the intercept including the standard rate constant under experimental conditions.[30]

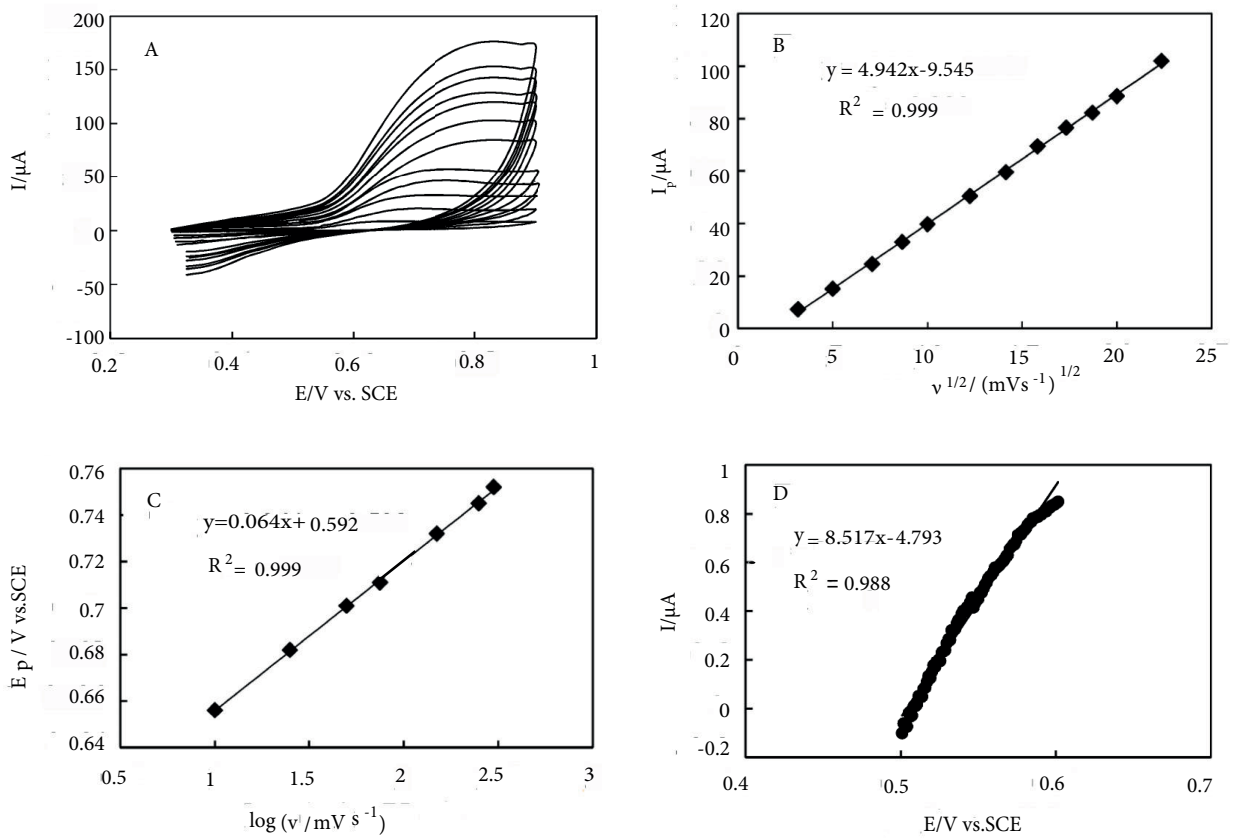

Figure 5. A) Cyclic voltammograms of MWCNTPE in 0.1 M PBS and 0.25 M KCl (pH 7) containing 0.2 mM deferasirox at scan rates of 10, 25, 50, 75, 100, 150, 200, 250, 300, 350, 400, and 500 mV s^{-1}. B) Plot of variations of peak currents (I_p) versus $\nu^{1/2}$. C) Plot of variations of peak potentials (E_p) versus log ν. D) Tafel plot obtained from currentpotential curves recorded at the MWCNTPE in the presence of 0.2 mM deferasirox at the scan rate of 20 mV s^{-1} at pH 7.

Based on Eq. (1), the slope of E_P as a function of log ν (Figure 5C) was found to be 64 mV/decade; thus, the Tafel slope was $b = 2 \times 64 = 128$ mV, which gave 0.46 for $(1 - \alpha) \quad n_a$. We also determined the value of $(1 - \alpha) \quad n_a$ using another method. A Tafel plot was constructed using background-corrected data from the rising part of the current–voltage curve at the scan rate of 20 mV s^{-1} (Figure 5D). For 0.2 mM deferasirox, a slope of 8.5 $(V/decade)^{-1}$ was witnessed, which gave a value of approximately 0.46 for $(1 - \alpha) \quad n_a$.

By assuming $\alpha = 0.5$, the value of n_a from two different methods was obtained to be 1.

2.6. Calculation of diffusion coefficient (D)

Chronoamperometry, as an effective electroanalytical method, was used for the evaluation of the diffusion coefficient of deferasirox. For this purpose, the Cottrell equation was used: [18,31,32]

$$\pi\tau i = \frac{nfAcD^{1/2}}{1/21/2}. \tag{2}$$

Figure 6 shows the current–time profiles obtained from setting the potential of the MWCNTPE working

electrode at 0.8 V in the presence of a) 1 mM, b) 1.5 mM, and c) 3 mM deferasirox. As can be seen, chronoamperograms of the analyte reached a steady state in approximately 3 s. Hence, we concluded that the response time of the electrode was 3 s. At long experimental times ($t > 1.5$ s, or $t^{-1/2} < 0.8$ s), where the electrocatalyzed oxidation rate of deferasirox exceeded that of deferasirox diffusion, the current demonstrated a diffusional nature. In this region, the graph of current I versus $t^{-1/2}$ gave a straight line (Figure 6 (inset A)), the slope of which was used to calculate the diffusion coefficient D of the analyte. From the graphs of these slopes versus c(Figure 6 (inset B)), D was found to be 1.8×10^{-6} cm^2 s^{-1} for deferasirox, which was comparable with previous reports.[17,18]

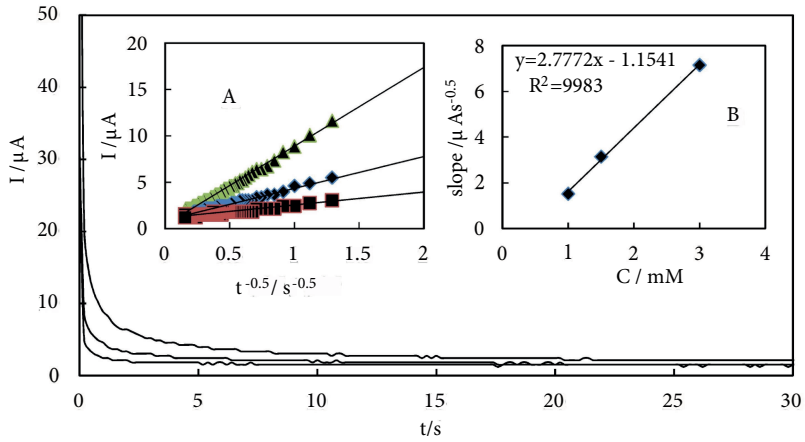

Figure 6. Chronoamperograms of MWCNTPE in the presence of (a) 1, (b) 1.5, and (c) 3 mM deferasirox in 0.1 M PBS and 0.25 M KCl with pH 7; potential step = 0.8 V. Inset A: Plot of variation of I versus $t^{-1/2}$, inset B: plot of slopes (obtained from inset A) versus c.

2.7. Analytical aspects

In this section, the capability of the MWCNTPE to determine deferasirox is described. Differential pulse voltammetry (DPV), a sensitive analytical technique, was used for the determination of deferasirox at low concentrations under optimum conditions.

2.7.1. Diagnostic performance

To assess the diagnostic performance of the proposed system, the MWCNTPE was immersed in a supporting electrolyte solution (pH 7) containing various concentrations of deferasirox and corresponding differential pulse voltammograms were recorded.

Figure 7A displays differential pulse voltammograms obtained from the addition of increasing amounts of deferasirox. The calibration graph shown in Figure 7B was linear in the range of 0.16–16.5 μM with a correlation coefficient of 0.998. The limit of detection was 0.1 μM, which was calculated by:

$$y_{LOD}(I) = y_B + 3S_{y/x}, \tag{3}$$

and the regression equation was:

$$y(I) = 0.170 + 0.3791c(\mu M), \tag{4}$$

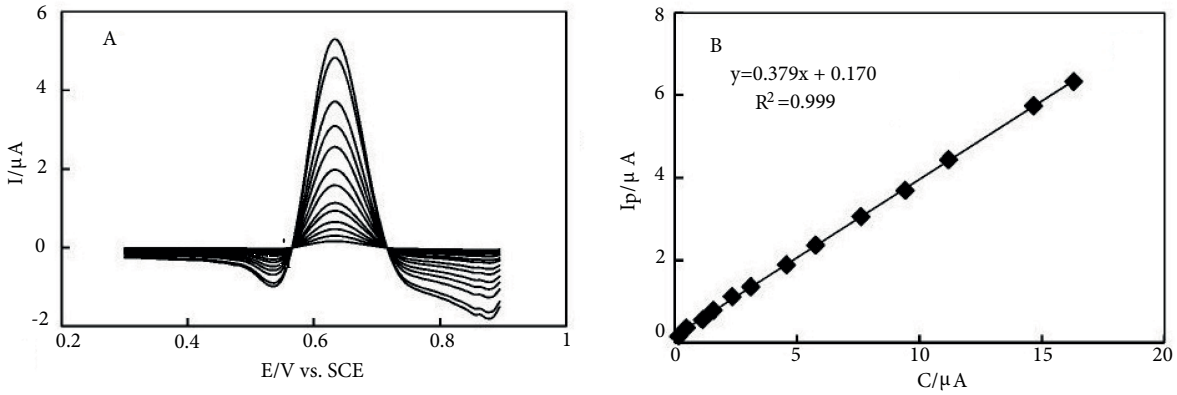

Figure 7. A) DPV results obtained from addition of increasing levels of deferasirox (0.16, 0.47, 1.14, 1.57, 2.34, 3.11, 4.56, 5.76, 7.61, 9.42, 11.19, 14.65, 16.3 μM) in 0.1 M PBS and 0.25 M KCl (pH 7). B) Calibration graph.

where y_B is the signal of the blank (here, the intercept of the calibration graph) and $S_{y/x}$ is the standard deviation of the blank (here, the SD of the calibration graph).[32] RSD was 1.8% for 4 successive determinations of 10 μM deferasirox solution, indicating remarkable reproducibility of the detection method.

2.7.2. Interference experiment

Interference experiments for detecting deferasirox in the presence of different species were conducted by recording voltammograms of deferasirox before and after the addition of these species and comparing their current responses. Deferasirox can coexist with some species such as lactose, glucose, F^-, uric acid, and dopamine in biological samples.

Interference experiments for the detection of deferasirox in the presence of 5 mM of each of these species were conducted by comparing current responses before and after the addition of the interferents to 0.1 M phosphate buffer solution containing 15 μM deferasirox.

The obtained results demonstrated that deferasirox peak currents before and after the addition of these species did not have significant differences and thus the above mentioned species did not interfere in the determination of deferasirox.

2.7.3. Determination of deferasirox in the presence of uric acid

Figure 8 shows differential pulse voltammograms of increasing amounts of deferasirox in the presence of an aliquot of uric acid. The calibration curve is presented in the inset of Figure 8. As shown in this figure, the calibration curve was linear in the concentration range of 0.83–16.9 μM. This study confirmed the applicability of the developed sensor for the determination of deferasirox in the presence of uric acid.

2.7.4. Determination of deferasirox in pharmaceutical and biological samples

To demonstrate the capability and potential applications of the prepared electrode for sample analysis, the proposed method was applied for the analysis of some real samples and the obtained results are presented in Table 2. The amounts of deferasirox in real samples were determined using the DPV technique and a standard addition method.

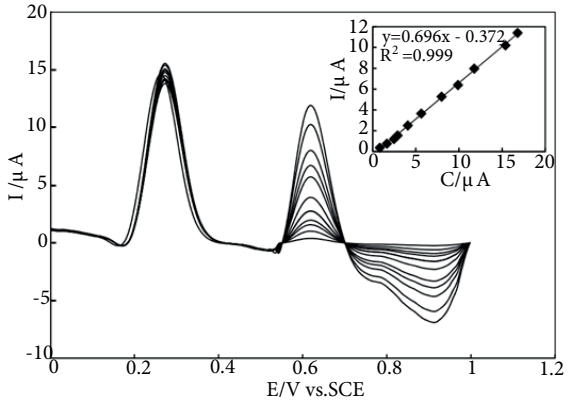

Figure 8. DPV results obtained from addition of increasing levels of deferasirox (0.83, 1.65, 2.47, 2.9, 4.08, 5.64, 8, 9.9, 11.77, 15.39, 16.79 μM) in 0.1 M PBS and 0.25 M KCl (pH 7) in the presence of 0.5 mM uric acid. Inset: Calibration graph.

Table 2. Results for the determination of deferasirox in pharmaceutical and biological samples.

Sample	Detected amount[a]	Spiked	Found amount[a]	RSD (%)	Recovery (%)
Deferasirox tablet, 125 mg	122.5 mg	100 mg	220.3 mg	2.1	97.8
Deferasirox tablet, 250 mg	243 mg	100 mg	340 mg	1.5	97
Deferasirox tablet, 500 mg	490 mg	200 mg	687.3 mg	1.2	98.6
Urine	_	1 μM	0.98 μM	1.6	98 %

[a]Average of three replicate determinations.

2.7.5. Comparative study of the performances of the existing methods

The electrochemical and nonelectrochemical performances of some previously published methods for the determination of deferasirox are summarized in Tables 3 and 4. As shown in these tables, the dynamic range of the proposed methods was comparable with those of other methods. The detection limit and sensitivity of the proposed method were also acceptable.

2.7.6. Stability of the sensor

Voltammograms of a specified concentration of deferasirox were recorded by the developed sensor about 7 and 30 days after electrode preparation. About 7 days after the preparation of electrode, the sensor retained about 98% of its initial sensitivity for the oxidation of deferasirox, while a month later, 93% of its initial efficiency was retained. Therefore, the MWCNTPE can be used as a sensor due to its long-term stability.

The peak current of freshly prepared deferasirox 1 week after the preparation of the electrode had not changed significantly and 95% of the efficiency was retained; however, the deferasirox solution was prepared freshly.

2.8. Conclusions

The MWCNTPE exhibited good electroactive characteristics for the electrooxidation of deferasirox. Compared to other options, this method had the advantages of low cost, simplicity, and high sensitivity and did not need time-consuming sample pretreatment steps.

Table 3. Comparison of the developed method with previously reported electrochemical techniques with different electrodes for the determination of deferasirox.

Electrochemical Method	Electrode	Linear range (μM)	Detection limit (μM)	Ref.
Amperometry	Carbon paste electrode modified with nanoparticles of Fe_2O_3 core-$NaCo[Fe(CN)_6]$ shell	0.23–5.8	0.91	[19]
Amperometry	Nickel oxyhydroxide-modified nickel electrode	132–1020	28	[17]
Amperometry	Cobalt oxide nanoflake-modified platinum electrode	99–650	6.67	[18]
Differential pulse voltammetry	Multiwall carbon nanotube paste electrode	0.15–16.5	0.1	This study

Table 4. Comparison of the developed method with previously reported nonelectrochemical techniques for the determination of deferasirox.

Method	Linear range (μM)	Detection limit (μM)	Ref.
UV–spectroscopy	13.35–80.01 μM (5 to 30 μg/mL)	1.07 μM (0.40 μg/mL)	[2]
RPHPLC–UV	2.67–16.02 μM (1 to 6 μg/mL)	0.27 μM (0.107 μg/mL)	[2]
UV–spectroscopy	5.4–32.4 μM (2 to 12 μg/mL)	0.66 μM (0.247 μg/mL)	[12]
Spectrofluorometry	0.005–5	1.5×10^{-3}	[10]
Differential pulse voltammetry	0.15–16.5	0.1	This study

The MWCNTPE that was used as a working electrode in this study possessed the advantages of both CPEs and nanomaterials. Preparation of this electrode was convenient and the nanotubes used in the manufacturing of the electrode caused the high sensitivity of this method. The electrochemical behavior of deferasirox was investigated by this electrode using CV and chronoamperometry. The results demonstrated that the rate-determining step was a one-electron process. Kinetic parameters such as D and α were also calculated. Finally, we used the DPV method to investigate the suitability of the electrode for the determination of deferasirox. The results indicated that the DPV method could be used as an effective technique for the determination of deferasirox for the MWCNTPE. The developed sensor was successfully used for the determination of deferasirox in urine and deferasirox tablet samples.

3. Experimental

3.1. Chemicals and reagents

Deferasirox, uric acid, and graphite powder were purchased from Merck. Multiwall carbon nanotubes (MWCNTs) of various concentric tube wall numbers (3–15) and lengths (1–10 μm) were purchased from Aldrich.

Supporting electrolyte solutions were prepared using 0.1 M phosphate (which was prepared by mixing stock solutions of K_2HPO_4 and KH_2PO_4 solution) and 0.25 M KCl and the pH was adjusted using saturated KOH and 12 M HCl solutions. All solutions were prepared with double-distilled water. All other chemicals were of analytical grade and were used without additional purification.

3.2. Apparatus

All voltammetry and chronoamperometry experiments were conducted using an AUTOLAB PGSTAT 30 electrochemical analysis system operated under the GPES 4.7 software package (Eco Chemie, the Netherlands). EIS experiments were performed using an EG&G Princeton Applied Research Model 263A Potentiostat/Galvanostat. A conventional three-electrode system comprising an MWCNTPE as working electrode, a saturated calomel electrode (SCE) as reference electrode, and a platinum wire as auxiliary electrode was used at room temperature. All potentials given in this paper were against the SCE. Measurements of pH were performed using a pH-meter (Metrohm-654) and scanning electron microscopy (SEM) images were recorded with a MIRA3 TESCAN field emission microscope.

3.3. Preparation of MWCNTPE and CPE

The MWCNTPE was prepared by thoroughly mixing 4.25 g of graphite powder and 0.75 g of MWCNTs with 1.8 mL of paraffin oil with a mortar and pestle. For preparing the CPE, 5 g of graphite powder was mixed with 1.8 mL of paraffin oil with a mortar and pestle.

The carbon pastes obtained from each of the above methods were packed into the hole of the electrode body. The surfaces of the electrodes were cleaned by sequential mechanical polishing with 800, 2000, 2500, and 3000 grit polishing papers and were then smoothed with a clean paper until shiny surfaces were obtained.

3.4. Real sample preparation

3.4.1. Deferasirox tablet sample

First, one deferasirox tablet was weighed carefully. Then five deferasirox tablets were powdered and aliquots equal to the weight of one tablet were weighed and transferred to a flask containing specified volumes of distilled water and were agitated for 5 min. The sample solutions were centrifuged for 15 min and were finally filtered through a filter paper (Whatman No. 42).

3.4.2. Spiked urine sample

For the preparation of a spiked urine solution, an aliquot amount of deferasirox was added to a specified volume of urine sample and was dissolved completely.

References

1. Desai, N.; Senta, R. *Journal of Taibah University for Science* **2015**, *9*, 245-251.
2. Somisetty, V. S. R.; Dhachinamoorthi, D.; Rahaman, S.; Rao, C. M. P. *Int. J. ChemTech. Res.* **2013**, *5*, 1861-1868.
3. Borgna-Pignatti, C.; Cappellini, M.; Stefano, P.; Vecchio, G.; Forni, G.; Gamberini, M.; Ghilardi, R.; Origa, R.; Piga, A.; Romeo, M. et al. *Ann. N. Y. Acad. Sci.* **2005**, *1054*, 40-47.
4. Borgna-Pignatti, C.; Vergine, G.; Lombardo, T.; Cappellini, M. D.; Cianciulli, P.; Maggio, A.; Renda, D.; Lai, M. E.; Mandas, A.; Forni, G. et al. *Br. J. Haematol.* **2004**, *124*, 114-117.

5. Porter, J. B. *Br. J. Haematol.* **2001**, *115*, 239-252.
6. Anandakumar, K.; Chinthala, R.; Subhash, V.; Jayamariappan, M. *J. Pharm. Res.* **2011**, *4*, 2998-3000.
7. Chakravarthy, V.; Gowrisankar, D. *J. Global Trends Pharm. Sci.* **2010**, *1*, 37-45.
8. Kaja, R. K.; Surendranath, K.; Radhakrishnanand, P.; Satish, J.; Satyanarayana, P. *Chromatographia* **2010**, *72*, 441-446.
9. Khan, M. A.; Sinha, S.; Todkar, M.; Parashar, V.; Reddy, K. S.; Kulkarni, U. *Int. J. Pharm. Biomed. Res.* **2011**, *2*, 128-134.
10. Manzoori, J. L.; Jouyban, A.; Amjadi, M.; Panahi-Azar, V.; Tamizi, E.; Vaez-Gharamaleki, J. *Luminescence* **2011**, *26*, 244-250.
11. Sambasivarao, V.; Phani, R.; Seetharaman, R.; Lakshmi, K. *IJPI's Journal of Analytical Chemistry* **2011**, *1*, 31-35.
12. Marathe, G. M.; Pande, V. V.; Patil, P. H.; Mutha, R. E.; Bari, S. B. *Indian Drugs* **2013**, *50*, 27-32.
13. Kissinger, P.; Heineman, W. R. *Laboratory Techniques in Electroanalytical Chemistry, Revised and Expanded.* CRC Press: Boca Raton, FL, USA, 1996.
14. Özkan, S. A.; Uslu, B.; Aboul-Enein, H. Y. *Crit. Rev. Anal. Chem.* **2003**, *33*, 155-181.
15. Smyth, M. R.; Vos, J. G. *Analytical Voltammetry.* Elsevier: Amsterdam, the Netherlands, 1992.
16. Wang, J. *Electroanalytical Techniques in Clinical Chemistry and Laboratory Medicine.* VCH: New York, NY, USA, 1996.
17. Hajjizadeh, M.; Jabbari, A.; Heli, H.; Moosavi-Movahedi, A.; Shafiee, A.; Karimian, K. *Anal. Biochem.* **2008**, *373*, 337-348.
18. Heli, H.; Yadegari, H.; Karimian, K. *J. Exp. Nanosci.* **2011**, *6*, 488-508.
19. Sattarahmady, N.; Heli, H. *Sens. Lett.* **2012**, *10*, 794-805.
20. Ensafi, A. A.; Maleh, H. K. *Int. J. Electrochem. Sci.* **2010**, *5*, 1484-1495.
21. Apetrei, C.; Rodriguez-Méndez, M.; Parra, V.; Gutierrez, F.; De Saja, J. *Sens. Actuators B Chem.* **2004**, *103*, 145-152.
22. Rodríguez-Méndez, M.; Gay, M.; Apetrei, C.; De Saja, J. *Electrochim. Acta* **2009**, *54*, 7033-7041.
23. Ruiz-Morales, J.; Canales-Vázquez, J.; Marrero-López, D.; Savvin, S.; Núnez, P.; Dos Santos-García, A.; Sánchez-Bautista, C.; Peña-Martínez, J. *Carbon* **2010**, *48*, 3964-3967.
24. Švancara, I.; Vytřas, K.; Barek, J.; Zima, J. *Crit. Rev. Anal. Chem.* **2001**, *31*, 311-45.
25. Ensafi, A. A.; Karimi-Maleh, H. *J. Electroanal. Chem.* **2010**, *640*, 75-83.
26. Beitollahi, H.; Karimi-Maleh, H.; Khabazzadeh, H. *Anal. Chem.* **2008**, *80*, 9848-9851.
27. Mazloum-Ardakani, M.; Beitollahi, H.; Ganjipour, B.; Naeimi, H. *Int. J. Electrochem. Sci.* **2010**, *5*, 531-546.
28. Norouzi, P.; Faridbod, F.; Larijani, B.; Ganjali, M. R. *Int. J. Electrochem. Sci.* **2010**, *5*, 1213-1224.
29. Treacy, M. J.; Ebbesen, T.; Gibson, J. *Nature* **1996**, *381*, 678-680.
30. Bard, A. J.; Faulkner, I. R. *Electrochemical Methods, Fundamentals and Applications.* Wiley: New York, NY, USA, 2001.
31. Pournaghi-Azar, M. H.; Saadatirad, A. *J. Electroanal. Chem.* **2008**, *624*, 293-298.
32. Pournaghi-Azar, M. H.; Ahour, F. *Electroanalysis* **2010**, *22*, 2413-2420.